

Properties of Poly (isoprene) - Model Building in the Melt and in Solution

Roland Faller*

*Department of Chemical Engineering & Materials Science,
University of California-Davis, Davis, CA 95616, USA*

Dirk Reith†

Max-Planck-Institut für Polymerforschung, 55128 Mainz, Germany

Properties of 1,4-*trans* poly (isoprene) at ambient conditions are determined by simulations on two length scales based on two different models: a full-atomistic and a mesoscopic one. The models are linked via a mapping scheme such that one mesoscopic bead represents one chemical repeat unit. Melts as well as solutions of several chain lengths were investigated and mapped individually to the meso-scale. The resulting models are compared to each other. The meso-scale models could be simulated over a large variety of chain lengths and time-scales relevant for experimental comparison. Concerning static properties, we determined the persistence length of our systems and the scaling behavior of the radius of gyration. The latter was compared to experiments and the agreement is satisfactory. Furthermore, we find deviations from Rouse dynamics at all chain lengths at ambient conditions.

I. INTRODUCTION

Poly (isoprene), better known as rubber, is one of the most commonly used polymers. Its natural form, kautschuk, is highly abundant in nature and for technological purposes, synthetic variations are easily industrially polymerised from isoprene [1]. As an elastomer, its rich field of technical applications comprises tires, textiles, or cable coatings [2]. Still, some of its static as well as dynamic properties are still not understood on a microscopic basis.

The time- and length-scales important for the investigation of polymeric materials generally cover a wide range - from Angstroms and picoseconds to millimeters and eventually hours. There is no hope to capture all important quantities of a system with one single model. Thus, computational methods have to be developed to use the information of more detailed models as an input for coarser models allowing to investigate larger systems. The most prominent example is the step from quantum chemistry (based on Schroedinger's equation) to semi-empirical atomistic models (based on Newton's equation of motion). For many modern applications, however, this step is not sufficient. So, the mapping of atomistic systems to meso-scale systems (in which monomers, thought of as "super-atoms", are the smallest units of the simulation) became the focus of several studies.

Coarse-graining (CG) approaches have reached considerable attention over the last decades [3]. The basic idea of all CG schemes is to separate the system into fast and slow variables where the fast degrees of freedom are not of primary interest for the question under study. Thus, a model can be compiled containing the slow degrees of freedom only. Recently methods have become available to perform coarse graining in a polymer-specific and systematic way [4, 5, 6, 7]. We refer to a systematic procedure if the identity of the polymer is not lost during the mapping procedure. Moreover, the purpose of such techniques is to develop meso-scale models for the simulation of large systems of specific polymers. To ease the mapping procedure, two automatic optimization schemes have been developed by our coworkers and us: firstly a simplex algorithm technique [8?], and secondly the iterative Boltzmann inversion method which directly targets the problem of structure differences with a physically motivated approach [10]. Similar ideas have been applied to reproduce experimental data in atomistic simulations [11].

The goal we pursue here is that two models on different length scales should produce the same distribution functions on the larger of the two length scales. Then, we can regard them representing the same polymer. Due to its rich applications, we take poly (isoprene) as an example. Additionally we point out some differences to recent findings in studies of semi-generic bead-spring models incorporating stiffness as the only local characteristics [12, 13].

* Electronic Mail: rfaller@ucdavis.edu

† Present address: DaimlerChrysler AG, HPC G202, Fronaeckerstr. 40, D-71059 Sindelfingen, Germany

II. INVESTIGATIONS WITH ATOMISTIC DETAIL

As a basis for our mapping procedure we need atomistic simulations with good accuracy. We performed simulations with appropriately designed force-fields reproducing the atomistic structure and the thermodynamics very reliably.

A. Melt Investigations

The atomistic melt simulations have been described in detail in reference [14]. Here, we briefly summarize the main characteristics. The simulation box contains 100 oligomers of average length 10 monomers. All chains represent *trans*-poly (isoprene) (cf. Figure 1). We use a self-developed all-atom force-field resulting in 132 interaction sites for a 10-mer [14]; every atom is represented by one interaction site (cf. Tables I-III). The simulations lasted for 1 to 2 ns at ambient conditions ($T = 300$ K, $p = 101.3$ kPa), cf. Table IV. The model is capable of describing local reorientation functions in comparison to NMR measurements and reproduces reasonably the melt structure factor of poly (isoprene) [14, 15].

Atoms connected by any bonding potential did not interact by the Lennard-Jones potential. Additionally, the following non-bonded interactions were excluded: all within one monomer, and all C–C, C–H and H–H interactions between the second half of the carbons of one monomer (atoms C₃, C₄, and C₅) and the first half of its following neighbor (C₁ and C₂) including the hydrogens connected to them.

Constant temperature and pressure are ensured using Berendsen’s method [16] with time constants 0.2 ps for temperature and 8 ps for pressure, respectively. The pressure coupling using a compressibility of 2×10^{-7} kPa⁻¹ was employed for the three Cartesian directions independently. All simulations were performed using the YASP molecular simulation package [17] with a time-step of 1 fs and a cutoff for the non-bonded interactions at 0.9 nm. Configurations were saved every picosecond. No charges were used through the simulations.

B. Atomistic Simulations of Poly (isoprene) in Solution of Cyclohexane

For the atomistic simulations of *trans*-PI in cyclohexane we used the same force-field as in the melt simulations except that only interactions up to 1 – 4 interactions (inclusive) are excluded. The cyclohexane force-field was developed using the automatic simplex method [11] and tested in the dynamics of mixtures of cyclohexene and cyclohexane [18]. For this study we augmented the cyclohexane force-field with torsion potentials along the ring in order to avoid inadvertent flipping between the chair and boat configuration [19]. The densities of the solutions increase slightly with concentration of polymer (Tab. V). They are very close to the density of pure cyclohexane without torsions (767.7 kg/m³) [11, 18], which in turn was optimized against experimental data. We did not reoptimize the Lennard-Jones parameters. Therefore the pure cyclohexane system has a slightly lower density as the molecules are less flexible and less spherical due to the torsions. In order to decide on the quality of the solvent the radius of gyration

$$R_G = \sqrt{\frac{\sum_i (m_i r_i^2)}{\sum_i m_i}}, \quad \vec{r}_i = \vec{R}_i - \langle \vec{R}_i \rangle \quad (1)$$

and the end-to-end length are important characteristics. The mean square end-to-end distance $\sqrt{\langle R_{e-e}^2 \rangle}$ is measured between the terminal carbons of the chain. Additionally the hydrodynamic radius R_H was calculated as the first inverse moment of the distance vectors [20]:

$$\frac{1}{R_H} = \frac{1}{N^2} \left\langle \sum_{i \neq j} \frac{1}{r_{ij}} \right\rangle. \quad (2)$$

Here, N represents the number of monomers of the chain and r_{ij} the distance between two arbitrarily chosen superatoms i and j .

We do not find a systematic variation of the radius of gyration with concentration. In the system with two chains in a solvent of 500 molecules the two chains behave differently whereas in the higher concentrated systems the radii of gyration are very close although they were also started with the same initial configurations as the other two chain system. The auto-correlation functions of the gyration radii, however, decays on the scale of less than a hundred pico-seconds. Thus, the systems are equilibrated even though the error bars are quite large. In order to decrease them substantially much larger simulations would be necessary. This was not the purpose of the atomistic simulations as the long time-scales are left to the coarse-grained model to be developed here.

In Figure 2 we show the decay of the reorientation correlation function of the end-to-end vector of the whole chains in solution. We see that this function overall follows an exponential tendency and the correlation time is in the order of 2 – 4 ns. This supports once again the assumption of equilibration. Additionally the overall reorientation becomes slower with increasing concentration. The dynamics of the solvent is found to slow down and become more anisotropic with increasing concentration [19].

III. THE MAPPING PROCEDURE

The mapping procedure is the same for both the melt and the solution system. It has already been described in full detail in reference [10], so we limit ourselves to a short summary. Distribution functions from atomistic simulations are the basis of the mapping, since the mesoscale model is optimized against them. In this study, M1 (for the melt) and the combination of S1 and S3 (for the solution) were chosen as parent atomistic simulations. The mapping itself is illustrated in Figure 1. Each chemical repeat unit is replaced by one super-atom (interaction center), located in the middle of the atomistic bond between successive chemical repeat units. Consequently an atomistic N -mer will be coarse grained to a $N - 1$ -mer. This is meaningful because the such mapped super-atoms are much more spherical compared to the case in which one would have chosen the center of mass of the real monomer. The advantage is that the mapped chains generate well distinguishable peaks for the various intramolecular distributions. Especially when applying the model to longer chains, the error introduced due to the missing rests are negligible.

In this contribution, we use exclusively the pressure-corrected CG force field which has been optimized by the Inverted Boltzmann method. It is fully described in Reference [10]. The idea, however, shall shortly be illustrated here. The Inverted Boltzmann method utilizes the differences in the potentials of mean force between the distribution functions generated from a guessed potential and the true distribution functions to improve the effective potential successively. Imagine we would like to derive an effective non-bonded potential $V_\infty(r)$ from a given tabulated start potential $V_0(r)$, targeting to match the radial distribution function $g_\infty(r)$. Simulating our system with $V_0(r)$ will yield a corresponding $g_0(r)$ which is different from $g_\infty(r)$. The potential needs to be improved, which is done by a correction term $-k_B T \ln \left(\frac{g_0(r)}{g(r)} \right)$. This step can be iterated as follows by:

$$V_{j+1}(r) = V_j(r) - k_B T \ln \left(\frac{g_j(r)}{g(r)} \right) \quad (3)$$

until

$$f_{\text{target}} = \int_{r_{\text{min}}}^{r_{\text{max}}} \omega(r) (g_\infty(r) - g_j(r))^2 dr . \quad (4)$$

falls below an initially specified threshold. (We apply $w(r) = \exp(-r)$ as weighting function in order to additionally penalize deviations at small distances.) Pressure corrections can be introduced in polymer systems by adding a weak linear potential term to the attractive outer part of $V_j(r)$. One can then post-optimize the structure of the system according to the above scheme in turn with occasional linear additions until the pressure matches the one from the atomistic system, too.

IV. MESOSCALE SIMULATIONS

A. Technical Simulation Details

Both Brownian Dynamics (BD, for the melt) and Monte Carlo (MC, for the solution) programs have been applied. All BD runs were performed in the NVT ensemble, with values for density and temperature corresponding to the values of the parent atomistic simulation. The systems consisted of an orthorhombic box employing periodic boundary conditions. Langevin equations of motion were integrated by the velocity Verlet algorithm with a time step $\Delta t = 0.01\tau$ [21] at a dimensionless temperature of $T^* = 1$. This temperature was maintained by the Langevin thermostat with friction constant $\Gamma = 0.5\tau^{-1}$ [22]. For the MC simulations representing the solution case, a single chain program was used [23]. Here, 10^5 accepted warm-up moves were carried out before a production run of 10^6 accepted moves was started. For analysis, every 500th configuration was stored, both in BD and MC simulations.

B. Static properties in the melt and in solution

The results of the CG simulations are summarized in Table VI in case of the poly (isoprene) melts and in Table VII in case of the solutions. For both, the radius of gyration R_G and the hydrodynamic radius R_H is correctly reproduced compared to the values of the parent atomistic simulations (within standard errors).

Extensive Brownian Dynamics simulations were carried out to investigate the static and the dynamic behavior of poly (isoprene) melts. The coincidence (within statistical fluctuations) of the values for D_{center} and D_{com} , representing the diffusion coefficient of the central monomer of the chain and their center of mass, respectively, shows that the system is fully equilibrated. Let us here concentrate on the static properties. In Table VI we list the values for the radius of gyration R_G , the hydrodynamic radius R_H , their ratio and the ratio R_e^2/R_G^2 which provide information about the extension of the chains. The scaling behavior of R_G is shown in Figure 3. A fit for $N \geq 35$ yields a scaling exponent of $\nu = 0.53$, which is slightly larger than the ideal value for melts of $\nu_\theta = 0.5$, suggesting that the chains are not sufficiently close to the limit of infinitely long chains. This is also supported by the ratio R_G/R_H which is well below the infinite limit of around 1.5. The fact that $R_e^2/R_G^2 = 6.0$ holds for all chain lengths, however, shows that the static behavior corresponds to random walks.

Table VII holds the results of the dissolved poly (isoprene) systems. Since we applied MC, static properties are listed exclusively. The scaling behavior of R_G is also presented in Figure 3. With a fit for the same region as in the melt case ($N \geq 35$) we obtain a scaling exponent of $\nu = 0.60$. This is only slightly larger than the theoretical value $\nu_{gs} = 0.588$ for polymers in good solvents due to the finite chain length. The ratio R_e^2/R_G^2 decreases monotonically with chain length. This indicates that the intramolecular interactions of poly (isoprene) in the *trans* state locally stretch the chains.

To the best of our knowledge only chain size measurements of *cis*-poly (isoprene) in solution of cyclohexane have been performed [24, 25]. Our data coincides within the order of magnitude with the extrapolated experimental data of Tsunashima *et al.* to our longest chains. Applying their relation for the gyration radius we calculate 2.76 nm for a chain length of 100 monomers in Θ -solution. This is almost exactly our value for the chains of this length in the melt where also random walk statistics is supposed to apply. Davidson *et al.* measured the radius of gyration of a mixture of *cis* and *trans* poly (isoprene) under good solvent conditions by various techniques including wide angle light scattering for molecular weight range of 112,000 g/mol and higher.[24] This corresponds to chain lengths of 1650 monomers and longer. Extrapolating the simulation data to the two shortest chains experimentally available we get 23.7 nm for 112,000 g/mol compared to 17.7 nm experimentally and 26.5 nm for 164,000 g/mol against 19.4 nm experimentally. Thus, we overestimate the gyration radii by about 35%. However, one has to keep in mind that the experimentally investigated system contains a mixture of the *trans* and *cis* conformer. The experimentally observed scaling exponent is 0.545 and therefore lower than our exponent of 0.6 and also lower than the theoretically predicted exponent of 0.588.

Next, the persistence length l_p of poly (isoprene) was estimated by the decay of the orientation correlation along the chain backbone. The point where this correlation arrives at $y = \exp(-1)$ is a good approximation of l_p

$$\langle \vec{u}_k(n+j) \vec{u}_k(n) \rangle = \exp\left(-\frac{j l_b}{l_p}\right). \quad (5)$$

Here, l_b is the bond length and $\vec{u}_k(n)$ represents the unit vector along the chain, centered at monomer n and pointing to monomer k . The result is shown in Figure 4. The bonds are completely decorrelated beyond the fourth neighbor for the melt. For the persistence length, $l_p \approx 1.25 l_b (= 0.59 \text{ nm})$ can be estimated. As expected, this is independent of chain lengths, as all curves fall on top of each other. The same holds for the solution case. Here the persistence length could be estimated to be $l_p \approx 2.7 l_b (= 1.27 \text{ nm})$, i.e. more than twice as large as for the melt. So, the concentration of poly (isoprene) chains has a strong influence on the intrachain statistics. The dense packing in the melt favors a quick decorrelation between neighboring chain monomers.

Finally, we can compare some of the above results to data for a melt of generic bead-spring chains with bond-angle stiffness [15]. It has already been used to successfully map the dynamic behavior of atomistic poly (isoprene) the meso-scale [13], even though it just comprised one simple bond angle potential in addition to a FENE bead spring interaction for the intramolecular part:

$$V_{\text{angle}} = x \cdot [1 + \vec{u}_j \cdot \vec{u}_{j+1}] k_B T. \quad (6)$$

The vector \vec{u} corresponds to a normalized bond vector and x is the force constant to determine the stiffness. The scalar product corresponds to the cosine of the angle along the backbone. The comparison of static properties of the two models is presented in Table VIII. One observes that most properties yield similar values, in case of R_G , R_e^2/R_G^2 , and l_p even within statistical error. However, the end-to-end distances deviate more strongly, showing that

the realistic poly (isoprene) chains are more coiled than generic chains. This is also reflected in the Kuhn segment length l_K , which defines the distance beyond which one expects universal chain behavior:

$$l_K = \frac{\langle \vec{R}_e^2 \rangle}{R_e^{(\max)}} = \frac{\langle \vec{R}_e^2 \rangle}{(N-1) l_b} = C_\infty l_b. \quad (7)$$

It is significantly shorter for the realistic model compared to the generic one. A reason for that could be the missing torsional potential in the latter. Also, the dynamical behavior turns out to differ significantly, as will be shown in the next section.

Although the mesoscopic model is optimized against the atomistic structure, some structural differences remain. Comparing the pair distribution functions of centers-of-mass of whole chains (cf. Figure 5) we see that the mesoscopic model chains show less structure on short distances. The mesoscopic 9-mers show just a correlation hole whereas the atomistic 10-mers exhibit a structured correlation hole. Moreover we see the strong difference between a mesoscopic 9-mer and a 50-mer. In the latter case the correlation hole is much less pronounced. This can be understood as the bigger a chain becomes the less volume of its ellipsoid of gyration it actually occupies and the more overlap of such ellipsoids is possible.

C. Dynamical Properties in the melt

The Rouse model [26] is widely accepted for the dynamics of short flexible chains in the melt. The assumptions it is based on are the screening of excluded volume and that all local intra-chain interactions can be mapped onto a Kuhn segment length [27]. Poly (isoprene) has been experimentally tested against the Rouse model [28] and the agreement was not too good at room temperature. Simulations at the atomistic model found for the oligomers of length 10 a reasonable description by the Rouse model at the elevated temperature of $T = 413$ K [13].

For long chains deviations from the Rouse model are expected due to mutual topological constraining of chains. Such deviations could then be attributed to entanglements since recently it has been shown that even a weak presence of stiffness can dramatically decrease the onset of entanglement influences [12].

Two observables are commonly used to decide on the validity of the Rouse model: the mean-squared displacements, and the so-called Rouse modes. Figure 6 shows the g_1 function which is defined as

$$g_1(t) = \langle (\vec{r}_i(t+t_0) - \vec{r}_i(t_0))^2 \rangle_{t_0}, \quad (8)$$

where $\vec{r}_i(t)$ denotes the position of the central monomer of a chain at a given time. The central monomer is chosen to suppress end-effects as good as possible. For short times ($t < \tau_R$) one expects all curves to fall on top of each other; τ_R is the Rouse time with all internal degrees of freedom are relaxed (below). At such short times the individual monomer does not yet have to drag the whole chain with it, but an increasing part. At $t \approx \tau_R(N)$ the different curves leave the master curve as the increasing neighborhood has reached the chain length. For longer chains Figure 6 shows clearly such a Rouse regime where $g_1(t) \propto t^{0.5}$. Additionally, for all chain lengths $N \leq 85$ we find the free diffusion limit $g_1(t) \propto t$ reached and therefore the systems equilibrated. This shows that the local dynamics is at least Rouse-like with the connectivity leading to a time dependent diffusion coefficient for $t < \tau_R$. This in turn leads to the sub-diffusive behavior observed. For longer chains the local regime lasts longer which clearly hints towards the connectivity behind the sub-diffusivity.

The actual Rouse model relies on the independence of the Fourier modes of the chains. We compare the decay of these Rouse modes \vec{X}_p

$$\vec{X}_p = \frac{1}{N} \sum_{i=0}^{N-1} \cos\left(\frac{\pi p(i + \frac{1}{2})}{N}\right) \vec{R}_i. \quad (9)$$

According to theory the curves for the different modes at a given chain length should collapse if the time and the correlation function are rescaled by the squared mode index [20]. For intermediate chain lengths we find this scaling to work reasonably well. For longer chain lengths, however, the higher modes are apparently faster than predicted by the Rouse model. This is first hint towards entanglements. It has been observed in simulations of other polymer models that especially the lower modes are likely to be the first to be influenced by entanglements [13, 29].

Table IX shows the Rouse time τ_R derived by an exponential fit to the first Rouse-Mode \vec{X}_1 . We clearly see finite chain length effects. For longer chains $N \geq 100$ these effects start to become weaker. Figure 7 compares the scaling for several chain lengths. This suggests that poly (isoprene) melts at room temperature do not completely behave according to Rouse theory.

We are not yet able to reach into the entanglement regime. Especially for the longest chains the scaling of the Rouse modes for different chain lengths onto each other apparently holds. It is interesting to note that we see finite chain length effects for chains of moderate length. Figure 7d is a way to tell oligomers from polymers as the self-similarity is obeyed in the polymer case. For oligomers the Rouse friction is still chain length dependent. This was not found in a recent study of model chains only incorporating stiffness. In that case the Rouse model was obeyed almost from the very beginning ($N > 15$). This is another important finding in the view of modeling long oligomers or short polymers. For chains with chemical identity we find a regime where the chain nature is already important but the generic polymer models are not yet valid.

V. CONCLUSIONS

Atomistic simulations of trans-poly (isoprene) in the melt and in solution have been simulated and independently coarse-grained to models with one interaction center per monomer. The local scale models are verified against experimental data where available. In the melt a slowdown of the dynamics is found as expected. For the solution we were able to equilibrate oligomers of length 15 monomers until the end-to-end reorientation correlation function decayed to less than about 30% of its initial value. Note, that we did not need heavy hardware resources to generate the statistical precision we present here.

The two independently coarse-grained models for solution and melt respectively are distinctly different. It is impossible to represent a chain in such strongly different environments on the coarse grained level with a generic potential. This is especially true as we aimed to get rid of the solvent completely in the solution case and melt and solution are very well known to behave strongly different in the long chain limit.

The coarse-grained models could be compared against well-known long polymer scaling theory. Additionally, comparison to experiments yielded a difference of 35%. The Rouse behavior is for this model recovered for chains of more than around 80 monomers. In summary, we find that the proposed coarse graining procedure allows us to produce models which are reliably reproducing properties of real polymers. We were not yet able to reach into the reptation regime.

Acknowledgements

Many fruitful discussions with Florian Müller-Plathe and Hendrik Meyer are gratefully acknowledged. RF wants to thank the Emmy-Noether program of the DFG (German Research Foundation) and DR wants to thank the BMBF (German Department of Research) Competence Center in Materials Simulation for financial support.

-
- [1] Stevens, M. P.; *Polymer chemistry: An introduction*; Oxford University Press; Oxford, New York; **1999**.
 - [2] Cowie, J. M. G.; *Chemie und Physik der synthetischen Polymere*; Vieweg; Braunschweig; **1997**.
 - [3] Baschnagel, J.; Binder, K.; Doruker, P.; Gusev, A. A.; Hahn, O.; Kremer, K.; Mattice, W. L.; Müller-Plathe, F.; Murat, M.; Paul, W.; Santos, S.; Suter, U. W.; Tries, V.; *Adv. Polymer Sci.* **2000**; *152*, 41–156.
 - [4] Tschöp, W.; Kremer, K.; Batoulis, J.; Bürger, T.; Hahn, O.; *Acta Polymer.* **1998**; *49*, 61–74.
 - [5] Reith, D.; Meyer, H.; Müller-Plathe, F.; *Macromolecules* **2001**; *34*, 2335–45.
 - [6] Reith, D.; Müller, B.; Müller-Plathe, F.; Wiegand, S.; *Structural properties of poly (acrylic acid) in aqueous solution*; **2002**; *J. Chem. Phys.* (in press).
 - [7] Akkermans, R. L. C.; Briels, W. J.; *J. Chem. Phys.* **2001**; *114*, 1020–1031.
 - [8] Meyer, H.; Biermann, O.; Faller, R.; Reith, D.; Müller-Plathe, F.; *J Chem Phys* **2000**; *113*, 6264–6275.
 - [9] Reith, D.; Meyer, H.; Müller-Plathe, F.; *Comp Phys Commun* **2002**; *148*, 299–313.
 - [10] Reith, D.; Pütz, M.; Müller-Plathe, F.; *Deriving Effective Meso-scale Coarse Graining Potentials from Atomistic Simulations*; **2002**; in preparation.
 - [11] Faller, R.; Schmitz, H.; Biermann, O.; Müller-Plathe, F.; *J. Comput. Chem.* **1999**; *20*, 1009–1017.
 - [12] Faller, R.; Müller-Plathe, F.; *ChemPhysChem* **2001**; *2*, 180–184.
 - [13] Faller, R.; Müller-Plathe, F.; *Polymer* **2002**; *43*, 621–628.
 - [14] Faller, R.; Müller-Plathe, F.; Doxastakis, M.; Theodorou, D.; *Macromolecules* **2001**; *34*, 1436–1448.
 - [15] Faller, R.; *Influence of Chain Stiffness on Structure and Dynamics of Polymers in the Melt*; PhD thesis; MPI für Polymerforschung and Universität Mainz; **2000**; published at <http://archimed.uni-mainz.de/pub/2000/0063>.
 - [16] Berendsen, H. J. C.; Postma, J. P. M.; van Gunsteren, W. F.; DiNola, A.; Haak, J. R.; *J. Chem. Phys.* **1984**; *81*, 3684–3690.
 - [17] Müller-Plathe, F.; *Comput. Phys. Commun.* **1993**; *78*, 77–94.

- [18] Schmitz, H.; Faller, R.; Müller-Plathe, F.; *J. Phys. Chem. B* **1999**; *103*, 9731–9737.
- [19] Faller, R.; *Phys Chem Chem Phys* **2002**; *4*, 2269–2272.
- [20] Doi, M.; Edwards, S. F.; *The Theory of Polymer Dynamics*; vol. 73 of *International Series of Monographs on Physics*; Clarendon Press; Oxford; **1986**.
- [21] Allen, M. P.; Tildesley, D. J.; *Computer Simulation of Liquids*; Clarendon Press; Oxford; **1987**.
- [22] Grest, G. S.; Kremer, K.; *Phys. Rev. A* **1986**; *33*, R3628–R3631.
- [23] Pütz, M.; Curro, J. G.; Grest, G. S.; *J Chem Phys* **2001**; *114*, 2847–60.
- [24] Davidson, N. S.; Fetters, L. J.; Funk, W. G.; Hadjichristidis, N.; Graessley, W. W.; *Macromolecules* **1987**; *20*, 2614–2619.
- [25] Tsunashima, Y.; Hirata, M.; Nemoto, N.; Kurata, M.; *Macromolecules* **1988**; *21*, 1107–1117.
- [26] Rouse, P. E.; *J. Chem. Phys.* **1953**; *21*, 1272–1280.
- [27] Kuhn, W.; *Kolloid Z.* **1934**; *68*, 2–15.
- [28] Floudas, G.; Reisinger, T.; *J Chem Phys* **1999**; *111*, 5201–5204.
- [29] Pütz, M.; *Dynamik von Polymerschmelzen und Quellverhalten ungeordneter Netzwerke*; PhD thesis; MPI für Polymerforschung and Universität Mainz; **1999**; published at <http://archimed.uni-mainz.de/pub/2000/0048>.
- [30] Ryckaert, J.-P.; Cicotti, G.; Berendsen, H. J. C.; *J. Comput. Phys.* **1977**; *23*, 327–341.

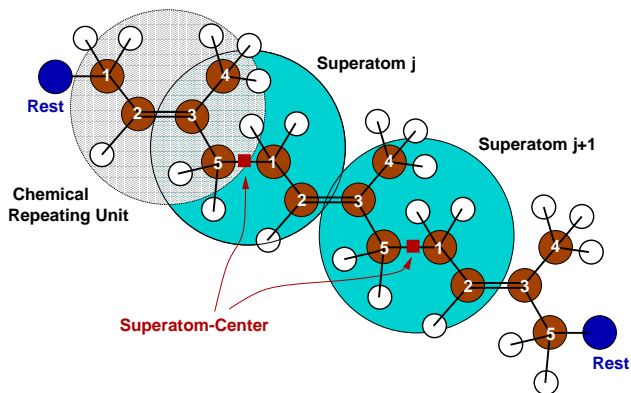


FIG. 1: Illustration of the mapping of *trans*-1,4-poly (isoprene) from the atomistic to the mesoscopic level. Each chemical repeat unit is represented by one super-atom. As center of these super-atoms, we choose the middle of the atomistic bond between two successive chemical repeat units. This is useful because the resulting mapped chains generate well distinguishable peaks for the various intramolec

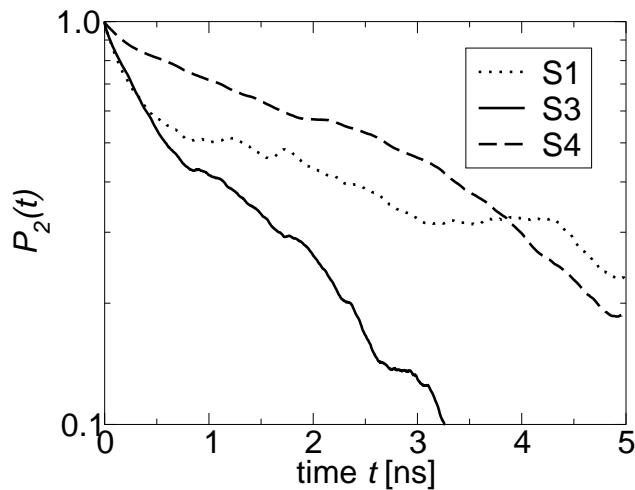


FIG. 2: Reorientation correlation function of whole chains in solution in semilogarithmic representation. We show the second Legendre polynomial P_2 of the reorientation angle. The shortcuts S1, S3, and S4 are defined in Table V.

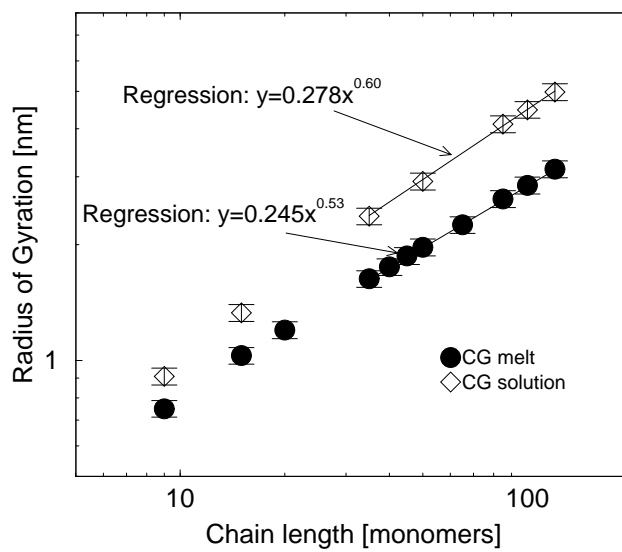


FIG. 3: Scaling behavior of CG poly (isoprene) chains in melt (filled circles) and solution (open diamonds).

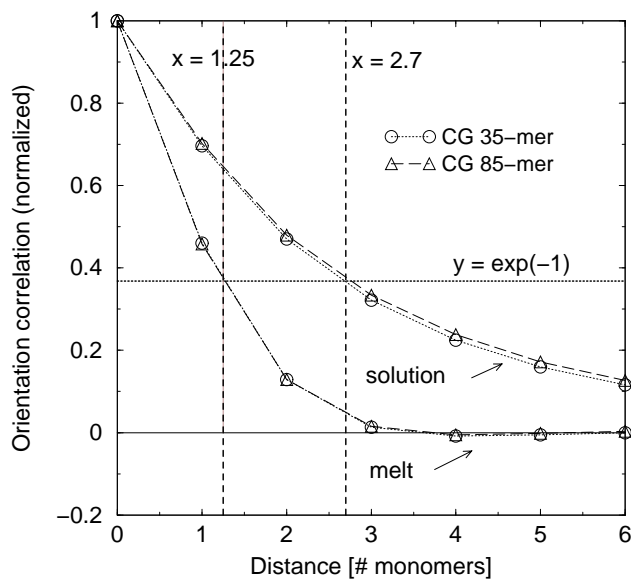


FIG. 4: Approximation of the persistence length l_p of some arbitrarily picked CG poly (isoprene) systems. Using eq. 5, the decay of the orientation correlation function to $y = \exp(-1)$ approximates l_p . In the melt, this yields $l_p \approx 1.25l_b$ and for the solution, $l_p \approx 2.7l_b$.

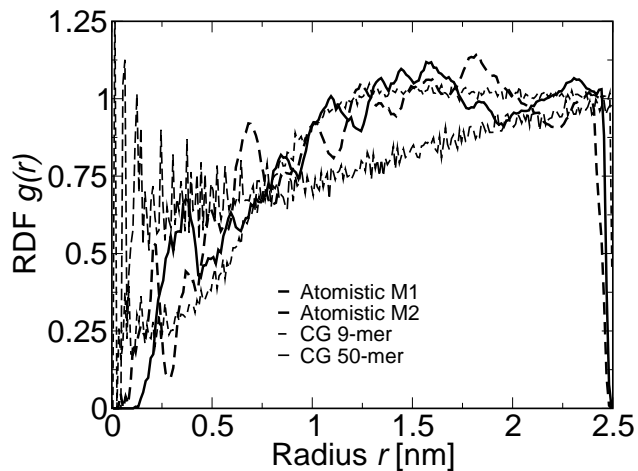


FIG. 5: Pair distribution function $g(r)$ for different chain models. We show two different atomistic 10-mers (M1 and M2), a mesoscopic 9-mer, and a mesoscopic 50-mer.

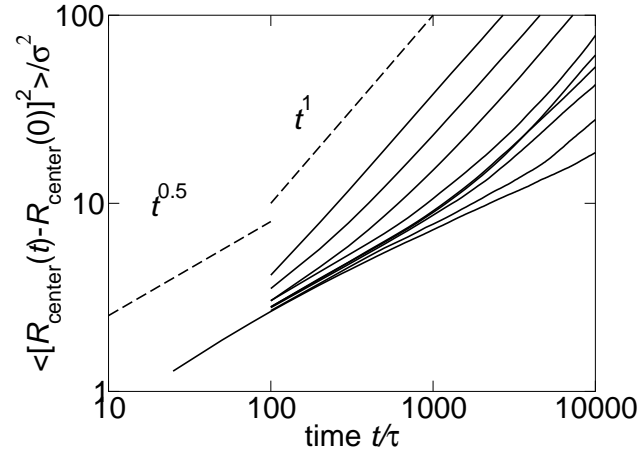


FIG. 6: The g_1 -function, mean-squared displacement of central monomers for the melt simulation at chain lengths $N = 9, 15, 20, 35, 40, 45, 50, 85, 120$ from top to bottom. As guides to the eye we show lines indicating $t^{0.5}$ and t^1 .

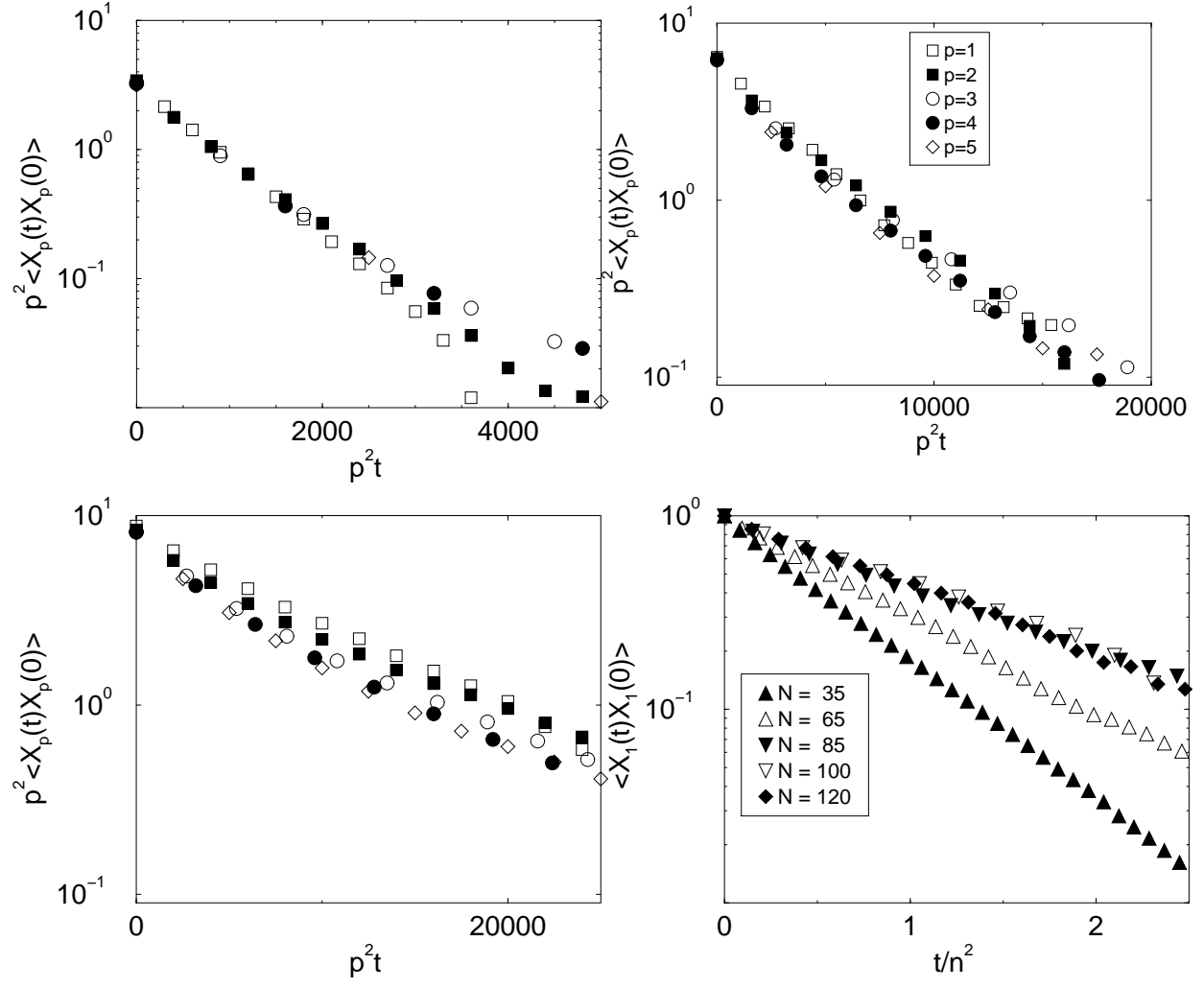


FIG. 7: Decay of the autocorrelation functions of the Rouse Modes for different chainlengths in Rouse scaling. Figure a) $N = 35$ b) $N = 65$, c) $N = 85$. The symbols are described in figure b. d) Comparison of the decay of the autocorrelation function for different chain lengths.

TABLE I: Angles (equilibrium values ϕ_0 and potential strength k) and bond lengths l_b for atomistic melt simulations of poly (isoprene). The bond lengths are constrained using SHAKE [30].

angle	ϕ_0	$k[\text{kJ}/(\text{mol} \cdot \text{rad}^2)]$	bond	$l_b[\text{nm}]$
$\text{C}_1 - \text{C}_2 - \text{C}_3$	128.7	250	$\text{C}_1 - \text{C}_2$	0.150
$\text{C}_2 - \text{C}_3 - \text{C}_4$	124.4	250	$\text{C}_2 = \text{C}_3$	0.1338
$\text{C}_2 - \text{C}_3 - \text{C}_5$	120.2	250	$\text{C}_3 - \text{C}_4$	0.151
$\text{C}_4 - \text{C}_3 - \text{C}_5$	115.4	250	$\text{C}_3 - \text{C}_5$	0.1515
$\text{C}_3 - \text{C}_5 - \text{C}_1$	114.5	250	$\text{C}_5 - \text{C}_1$	0.155
$\text{C}_5 - \text{C}_1 - \text{C}_2$	112.7	250	$\text{C} - \text{H}$	0.109
$\text{C} - \text{C}_{\text{sp}3} - \text{H}$	109.5	250		
$\text{C}_1 - \text{C}_2 - \text{H}$	114.4	250		
$\text{C}_3 - \text{C}_2 - \text{H}$	114.4	250		
$\text{H} - \text{C} - \text{H}$	109.5	250		

TABLE II: Force-field parameters of the non-bonded interactions for atomistic melt simulations of poly (isoprene). m is the atom mass, σ the interaction radius, and ϵ the interaction strength.

atom	m [amu]	σ [nm]	ϵ [kJ/mol]
C _{sp2}	12.01	0.321	0.313
C _{sp3}	12.01	0.311	0.313
H	1.00782	0.24	0.2189

TABLE III: Force-field parameters of the dihedral angles for atomistic melt simulations of poly (isoprene). The identifying numbers are found in figure 1

torsion equilibrium angle		barrier	periodicity
	τ_0 [degrees]	k_τ [kJ/mol]	i
1	0	5.2	1
1	0	-7.4	2
1	0	10.0	3
2	180	9.7	1
2	180	14.1	3
3	0	-21.1	1
3	0	-12.3	2
3	0	0.5	3

TABLE IV: Summary of the characteristics of the atomistic melt simulations.

system	T [K]	t_{sim} [ps]	$\frac{M_w}{M_n}$	ρ [kg/m ³]
<i>M1</i>	300	1184	1.00	890
<i>M2</i>	300	2012	1.05	917.4
<i>M3</i>	300	1737	1.05	916.8
<i>M3</i>	413	792	1.05	826

TABLE V: Thermodynamic and static properties of the solution. Details of the different systems and the numbers with which they are referenced in the following. N_P is the number of oligomers (C₇₅H₁₂₂) and N_C the number of cyclohexane molecules. c is the concentration in weight % polymer. t_{sim} is the simulated time for the systems.

system	N_P	N_C	c	ρ [kg/m ³]	t_{sim} [ns]	R_H [nm]	R_G [nm]	R_e^2/R_G^2
S0	0	500	0.0%	756.3	1.0	–	–	–
S1	1	250	4.6%	764.2	11.25	1.33 ± 0.12	1.21 ± 0.20	6.1
S2	1	500	2.4%	757.5	5.58	1.40 ± 0.05	1.26 ± 0.10	6.0
S3	2	500	4.6%	762.5	7.81	1.34 ± 0.10	1.23 ± 0.20	6.5
S4	2	250	8.9%	768.2	11.56	1.37 ± 0.09	1.29 ± 0.15	7.2

TABLE VI: Data of the mesoscopic Brownian Dynamics poly (isoprene) melt simulations. The pressure is stated in reduced units [21]. All systems are simulated at a temperature of $T = 300$ K and at a density of $\rho_p = 7.25$ monomers/nm³ and correspond to the atomistic simulation M1. The static properties come with a standard error of $\approx 5\%$, the dynamic properties with an error of $\approx 15\%$.

chain length N	9	15	20	35	40	45	50	65	85	100	120
number of chains N_c	100	150	150	100	150	150	80	130	50	120	100
pressure p^*	± 0.0	-0.01	-0.04	-0.15	-0.07	-0.08	-0.08	-0.08	-0.09	-0.09	-0.09
simulation time [10 ⁶ time steps]	3.0	4.0	4.0	7.2	6.0	6.0	8.0	6.0	8.0	6.0	6.0
R_G [nm]	0.75	1.03	1.20	1.63	1.75	1.87	1.97	2.25	2.63	2.85	3.14
R_H [nm]	1.11	1.19	1.27	1.50	1.60	1.65	1.69	1.98	1.98	2.21	2.42
R_G/R_H	0.68	0.86	0.94	1.09	1.10	1.13	1.17	1.14	1.33	1.29	1.30
R_e^2/R_G^2	6.0	6.0	6.0	6.0	6.0	6.0	6.0	6.0	6.0	6.0	6.0
D_{centre} [10 ⁻⁶ cm ² /s]	16.6	10.7	6.7	4.2	2.5	2.3	2.9	1.3	1.3	0.8	0.6
D_{com} [10 ⁻⁶ cm ² /s]	16.0	10.9	6.7	4.1	2.5	2.3	2.8	1.3	1.2	0.8	0.6

TABLE VII: Static properties (with standard errors of $\approx 5\%$) as obtained from Monte-Carlo simulations of mesoscopic poly (isoprene) solutions. The system density and temperature corresponds to the parent atomistic systems S1 and S3.

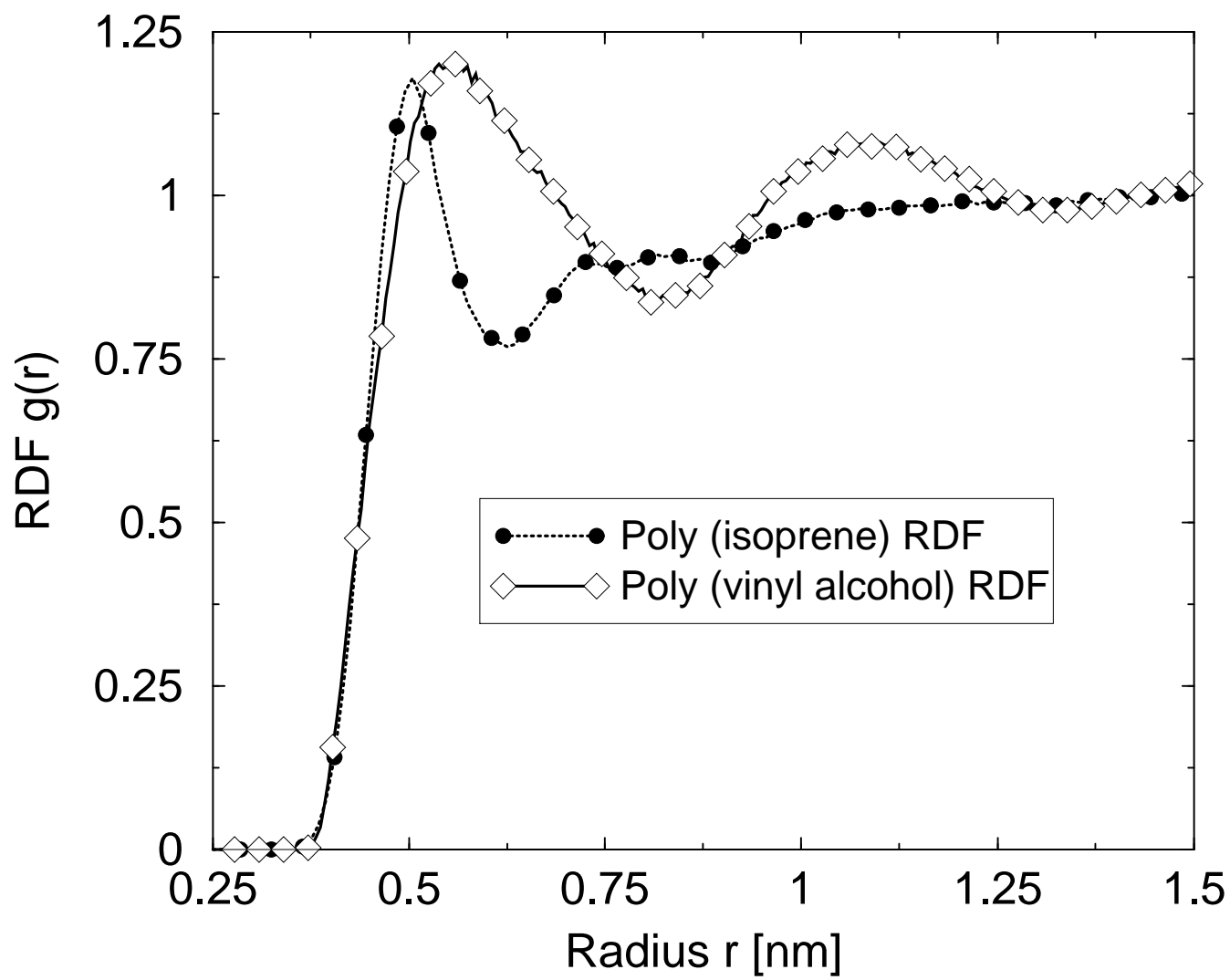
chain length N	9	15	35	50	85	100	120
R_G [nm]	0.91	1.33	2.37	2.92	4.11	4.48	4.98
R_H [nm]	1.23	1.40	1.98	2.32	3.06	3.31	3.63
R_G/R_H	0.74	0.95	1.20	1.26	1.34	1.35	1.37
R_e^2/R_G^2	7.3	7.1	6.7	6.5	6.5	6.4	6.4

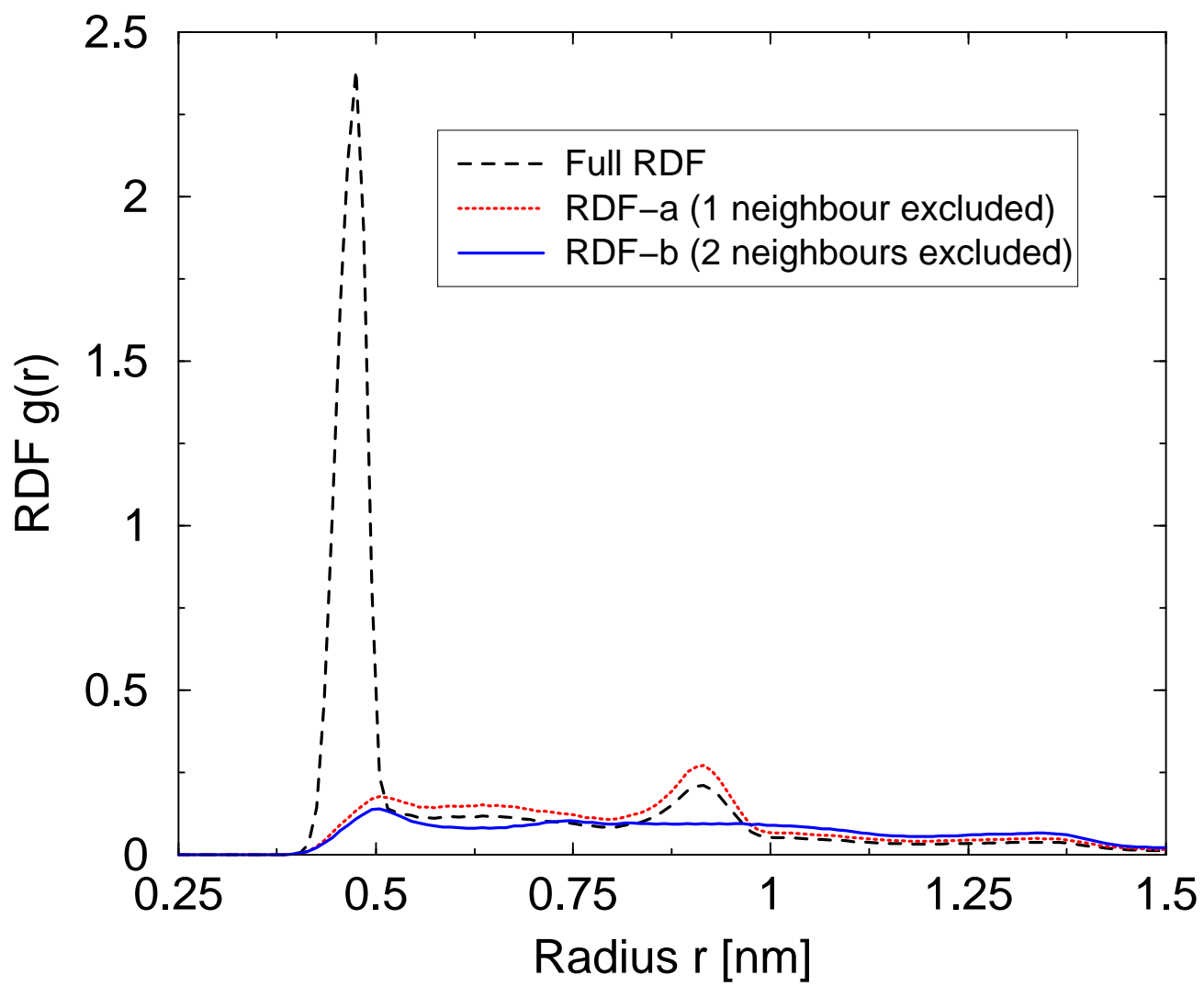
TABLE VIII: Results of some static properties for a realistic meso-scale model of poly (isoprene) in a melt and a more generic bead-spring model with bond-angle stiffness. R_G is the radius of gyration, R_e the end-to-end distance of the chain, l_p corresponds to the persistence length and l_K to the Kuhn segment length.

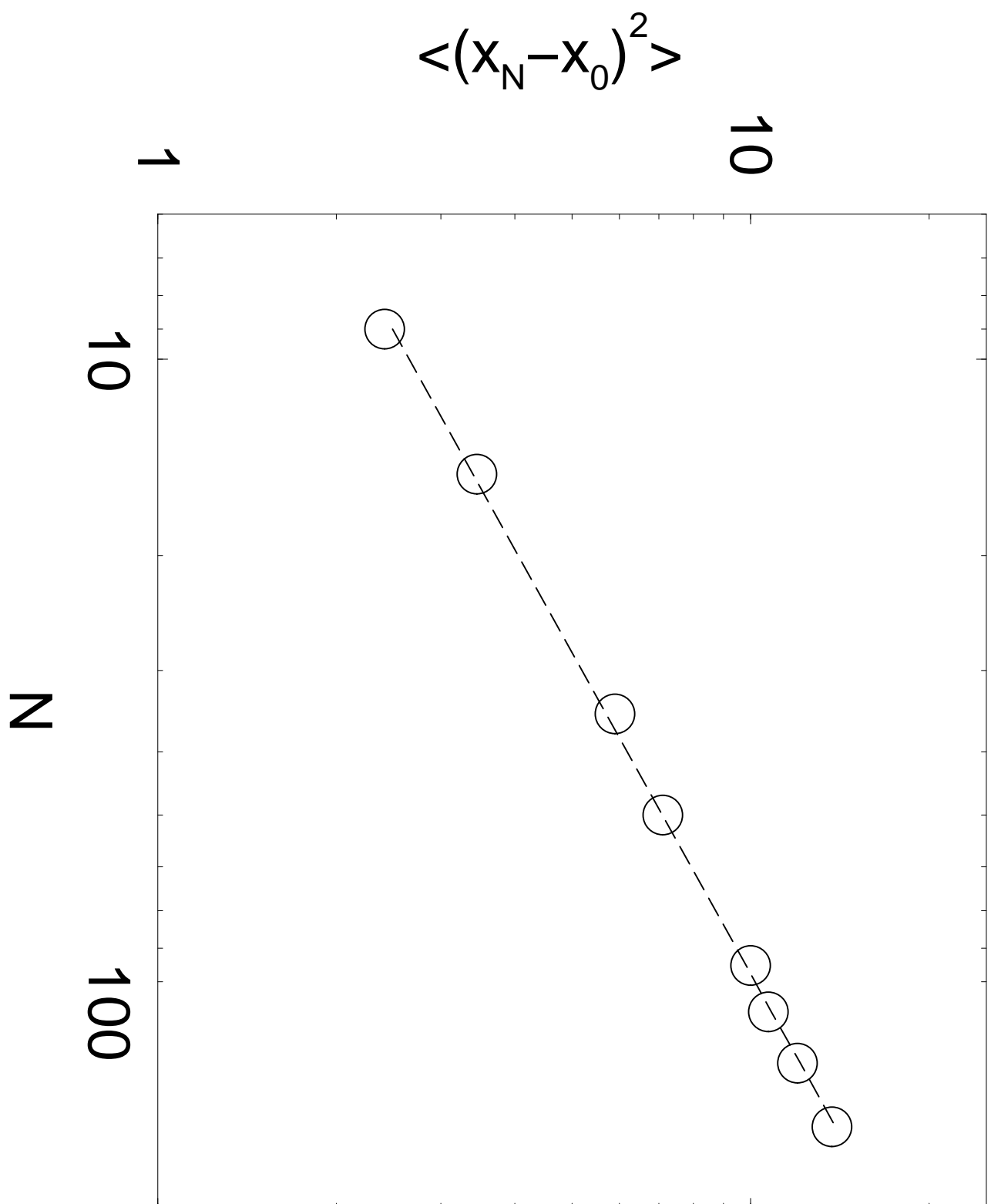
Melt Model	R_G [nm]	R_e^2 [nm ²]	R_e^2/R_G^2	l_p [monomers]	l_K [nm]
$x = 1.5, N = 20$ [15]	1.28	10.3	6.3	1.2	1.2
CG PI, $N = 20$	1.20	8.7	6.0	1.25	1.0
$x = 1.5, N = 50$ [15]	2.20	29.5	6.2	1.3	1.3
CG PI, $N = 50$	1.97	23.3	6.0	1.25	1.0

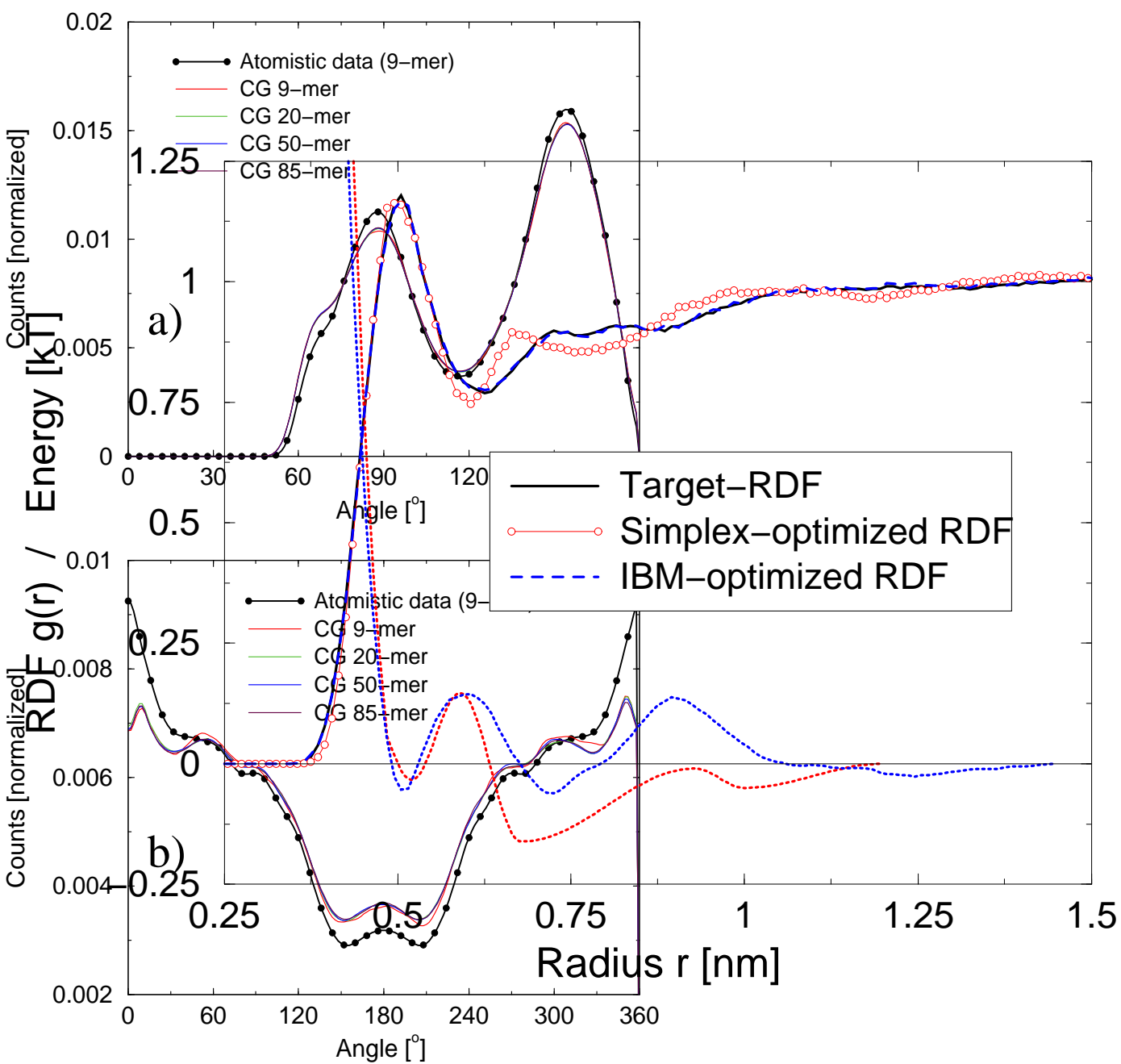
TABLE IX: Fits of the Rouse time using the decay of the first Rouse mode for different chain lengths.

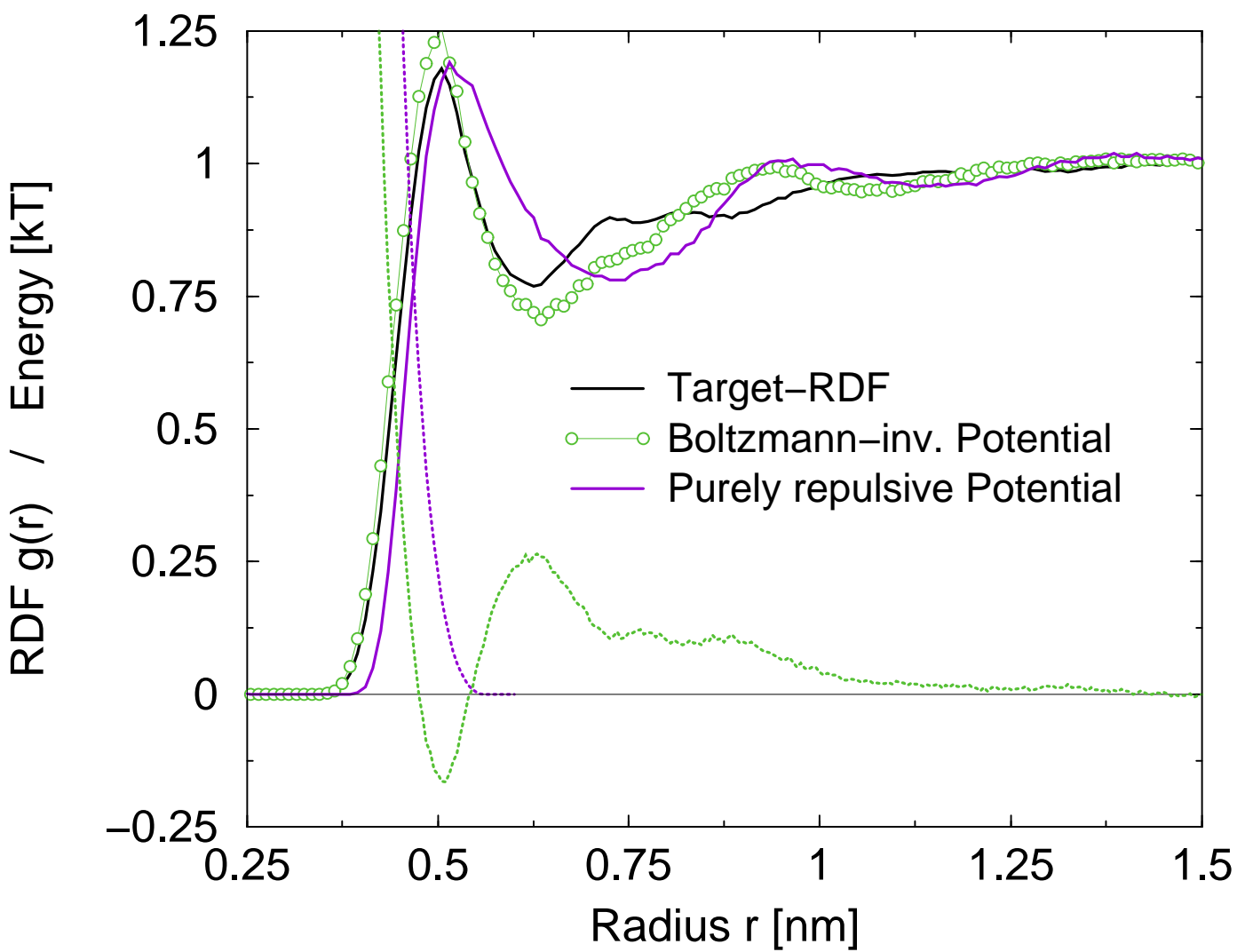
N	τ_R	τ_R/N^2
35	743	0.60
50	1946	0.78
65	3722	0.88
85	9300	1.29
100	13800	1.38
120	17700	1.23











UNIVERSITY OF
WISCONSIN
MADISON
